The Journal of Infectious Diseases

MAJOR ARTICLE

Genomic Evolution of Influenza A Virus During the 2024–2025 Season, the Johns Hopkins Health System: Antigenic Drift Reduces Serum Neutralization

David Villafuerte,[1] Amary Fall,[1] Elgin Akin,[2] Anne P. Werner,[2] Matthew Pinsley,[2] Yee Vue,[2] Omar Abdullah,[1] Ting Xuan Zhuang,[1] Julie M. Norton,[1] Richard E. Rothman,[3] Katherine Z. J. Fenstermacher,[3] C. Paul Morris,[4] Eili Klein,[3,5] Andrew Pekosz,[2] and Heba H. Mostafa[1]

[1]Department of Pathology, Division of Medical Microbiology, Johns Hopkins School of Medicine, Baltimore, Maryland, USA; [2]W.Harry Feinstone Department of Molecular Microbiology and Immunology, The Johns Hopkins Bloomberg School of Public Health, Baltimore, Maryland, USA; [3]Department of Emergency Medicine, Johns Hopkins School of Medicine, Baltimore, Maryland, USA; [4]Integrated Research Facility, Division of Clinical Research, National Institute of Allergy and Infectious Diseases, National Institutes of Health, Frederick, Maryland, USA; and [5]Center for Disease Dynamics, Economics, and Policy, Washington DC, USA

Background. Seasonal influenza causes significant global morbidity, mortality, and economic burden. Ongoing viral evolution can lead to vaccine mismatch and the emergence of antiviral resistance, highlighting the importance of genomic surveillance. The 2024–2025 influenza season was characterized by high incidence and increased hospitalizations.

Methods. We analyzed influenza A virus (IAV) genomes and clinical characteristics from the 2024–2025 season. Whole-genome sequencing was performed on 648 influenza A–positive clinical specimens collected between October 2024 and April 2025.

Results. Hemagglutinin (HA) sequences were recovered from 74.23% (481/648) of samples and used for subtyping and phylogenetic analysis. A(H1N1)pdm09 and A(H3N2) viruses cocirculated, representing 55.5% and 44.5% of cases, respectively. Among A(H1N1)pdm09 viruses, the HA1 substitution T120A, located near the Sa antigenic site, increased more than 2-fold compared with the prior season. Circulating A(H3N2) viruses belonged to multiple HA subclades and exhibited distinct amino acid substitutions at key antigenic sites. Neutralization assays using sera from individuals vaccinated with the 2024–2025 seasonal influenza vaccine demonstrated reduced neutralization of 3 dominant A(H1N1)pdm09 isolates and 2 A(H3N2) isolates compared with vaccine strains, consistent with antigenic drift. In addition, the neuraminidase substitution S247N, previously associated with reduced oseltamivir susceptibility, was detected in 13.9% of A(H1N1)pdm09 samples.

Conclusions. These findings demonstrate ongoing antigenic drift and the presence of antiviral resistance–associated mutations during the 2024–2025 influenza season, underscoring the need for continued genomic surveillance to guide vaccine and antiviral strategies.

Keywords. influenza; IAV; sequencing; viral genomic surveillance.

Influenza viruses cause annual epidemics with substantial morbidity and mortality. Among the 4 types—A, B, C, and D—only influenza A and B viruses (IAV and IBV) circulate widely in humans [1]. The IAV genus of the *Orthomyxoviridae* family is classified based on the surface glycoproteins hemagglutinin (HA) and neuraminidase (NA). Currently, 2 main subtypes—A(H1N1)pdm09 and A(H3N2)—circulate seasonally. These viruses disproportionately cause severe disease in high-risk groups, including elderly, young children, pregnant women, and individuals with chronic health conditions [2]. In the United States, the economic burden of influenza is significant and includes both direct healthcare costs and indirect impacts, largely due to missed workdays and reduced productivity [3].

Influenza virus genomes are segmented, negative-sense RNA. Mutations are introduced randomly across the genome during viral RNA replication, but when mutations alter antibody binding, they are designated as antigenic drift [1]. Such changes can lead to the selection of viruses capable of escaping preexisting population immunity. Therefore, tracking antigenic drift is essential for vaccine development and for monitoring vaccine effectiveness.

National surveillance efforts of influenza during the 2024–2025 season reported the most severe season since 2009–2010, with A(H1N1)pdm09 and A(H3N2) predominating followed by IBV-Victoria lineage (B/Victoria) [4, 5]. This study

Received 24 November 2025; accepted 30 January 2026; published online 4 February 2026

Correspondence: Andrew Pekosz, PhD, Department of Molecular Microbiology and Immunology, Johns Hopkins Bloomberg of Public Health, 615 North Wolfe Street, Room W2116, Baltimore, MD 21205-2103 (apekosz1@jhu.edu); Heba Mostafa, MD, PhD, D(ABMM), Department of Pathology, Johns Hopkins School of Medicine, Meyer B-121A, 600 N. Wolfe Street, Baltimore, MD 21287 (hmostaf2@jhmi.edu).

The Journal of Infectious Diseases®

https://doi.org/10.1093/infdis/jiag069

identifies the genomic mutations and prevalence of IAV strains at the Johns Hopkins Health System (JHHS) from October 2024 to April 2025, while the IBV surveillance data is discussed elsewhere [4]. Evidence of continued evolution of both A(H1N1)pdm09 and A(H3N2) viruses, with changes at antigenic sites, was obtained through phylogenetic and sequence analyses. Antigenic drift was documented in 3 A(H1N1)pdm09 and 2 A(H3N2) genotypes, providing biological evidence of reduced neutralization before and after vaccination using sera from a cohort of adult healthcare workers (HCWs).

METHODS

Ethical Considerations and Data Availability

The research was performed under protocols IRB00306448 and IRB00331396. Genomes are available in the Global Initiative on Sharing All Influenza Data (GISAID) database (accession numbers, Supplementary Table 1, HA and NA FASTA files, Supplementary Datasets 1–4). Serum samples were obtained from HCWs recruited from the Johns Hopkins Centers for Influenza Research and Response (JH-CEIRR) during the annual Johns Hopkins Hospital (JHH) employee influenza vaccination campaign in the Fall of 2024. Pre- and postvaccination (~28 days) human sera were collected from subjects, with written informed consent (IRB00288258). Viruses were isolated from deidentified IAV–positive samples (IRB00288258).

Study Population

Standard-of-care diagnostic influenza testing for the 5 JHHS hospitals was performed with either the Cepheid Xpert Xpress SARS-CoV-2/Flu/respiratory syncytial virus test (Sunnyvale, CA, USA) or the ePlex RP/RP2 respiratory panels (Roche Diagnostics, Indianapolis, IN, USA) [6, 7]. The Xpert Xpress assay targets the matrix (M), PB2, and PA segments for IAV [8]. The ePlex panels can subtype IAV as H1, H1–2009, and H3. Clinical samples were collected between October 2024 and April 2025 (sample selection was random, based on the availability after the standard-of-care testing and minimum sample volume required for nucleic acid extraction), and corresponding clinical and demographic metadata were extracted through the electronic medical charts, as previously described [9, 10].

Nucleic Acid Extraction and Whole-Genome Amplification

Nucleic acid was extracted using the Chemagic Viral RNA/DNA Kit following the manufacturer's instructions (Revvity, Waltham, MA, USA). The whole genomes of IAV were amplified as described previously [9, 10] using a multi-segment amplification approach developed by Zhou et al for IAV [11] and primer sets for IBV [12]. Library preparation was performed with influenza-adapted protocol that uses the NEBNext Artic SARS-CoV-2 Companion Kit (New England Biolabs, Ipswich, MA, USA), and sequencing was performed following the manufacturer's instructions, using R10.4.1 flow cells on a GridION or PromethION (Oxford Nanopore Technologies, Oxford, UK) [13].

Virus Genome Assembly and Phylogenetic Analysis

Fastq files were analyzed as previously described [9] using the FLU module of the Iterative Refinement Meta-Assembler. The alignment of genomes and reference sequences, downloaded from GISAID, was performed using the built-in alignment tool in Nextclade [14]. Quality control scores for sequences were assigned using the built-in pipeline available in Nextclade. Sequences with scores of 30 and above were excluded from sequence analysis. Sequences were viewed using BioEdit (version 7.7.1.0). Hemagglutinin and NA sequences with gaps were excluded from the analysis. The phylogenetic trees of HA and NA sequences, along with reference genomes from GISAID, were generated using the maximum likelihood method implemented in IQ-Tree (version 2.3.2). The ModelFinder, integrated within IQ-TREE2, was used to determine the best-fitted nucleotide substitution model. The robustness of the tree topology was tested with 1000 nonparametric bootstrap replicates. Phylogenetic tree visualization was performed using FigTree (version 1.4.4). Subclade assignments were initially made using Nextclade based on the HA segments and were confirmed through clustering patterns in the phylogenetic trees.

Amino acid substitutions (AAS) were assessed with Nextclade. For the 2024–2025 influenza season, Nextclade designated A/Wisconsin/588/2019 and A/Darwin/6/2021 to be suitable reference genomes for circulating A(H1N1)pdm09 and A(H3N2) viruses, respectively. To identify and quantify AAS, A(H1N1)pdm09 sequences from the 2024–2025 season were compared with the JHHS 2023–2024 sequences using an in-house script via Python (version 3.11.4) [15]. Strain A/Victoria/4897/2022 was the egg-based vaccine component used in 2023–2024 and 2024–2025 seasons and was used as a reference sequence for H1 HA comparative analyses (Supplementary Table 2 lists AAS of egg- and cell-based vaccine strains). An in-house Nextstrain build was used to perform a temporal analysis of JHHS genomes including entropy (as a measure of diversity) and amino acid prevalence analyses. These builds are interactively available at H1N1, https://nextstrain.org/groups/PekoszLab-Public/mostafa/iav24-25/h1n1/ha, and H3N2, https://nextstrain.org/groups/PekoszLab-Public/mostafa/iav24-25/h3n2/ha

Influenza A Isolation

Nasopharyngeal swabs from IAV–positive individuals were used for virus isolation on MDCK-SIAT-TMPRSS2 cells [16] as described previously [17]. TCID50 was performed on collected supernatants, and virus seed stocks were made when virus was detected at concentrations greater than 10^4 TCID50/mL. The A(H1N1)pdm09 clinical isolates obtained for this study

were JH25250, clade 5a.2a, subclade C.1.9; JH25260, clade 5a.2a.1, subclade D.3 (HA1: 113K); and JH25305, clade 5a.2a.1, subclade D.3 (HA1: 113R). The H3N2 clinical isolates obtained for this study were JH25588, clade 2a.3a, subclade J.2 (HA1: S145N, N158K), and JH25610, clade 2a.3a, subclade J.2 (HA1: T135K). Influenza vaccine strains A(H1N1)pdm09 (A/Victoria/4897/2022-egg) and H3N2 (A/California/122/2022-egg) were kindly provided by the US Centers for Disease Control and Prevention. Fifty percent tissue culture infectious dose was performed and calculated as previously described [17, 18].

Serum Neutralization Assay

Pre- and postvaccination human sera obtained through the JH-CEIRR vaccine study were used (age groups were 21–69; Supplementary Table 3). Neutralization assays were performed as previously detailed [17, 19]. The limit of detection (LOD) was determined to be the smallest possible area under the curve (AUC) or NT50 value generated, eg, when only 1 of 4 wells is protected at the first dilution in the full dilution series. Any samples that had no detectable neutralizing responses were set to be equal to one-half of the assay LOD for use in calculating geometric mean titers (GMTs).

RESULTS

Influenza Positivity, the JHHS

The 2024–2025 season showed increased positive influenza patients (Figure 1*A*) and hospital admissions (Figure 1*B*) when compared to the prior 6 influenza seasons. Notably, the overall positivity rate for the 2024–2025 season was higher and peaked in February, occurring later than the December peak that was observed in the 2023–2024 season [10] (Supplementary Figure 1). Between October 2024 and April 2025, a total of 5380 positive samples were detected from 57 488 samples collected across JHHS (9.4%). Of the 5380 IAV–positive samples, 648 (12%) were collected for whole-genome sequencing. Of these, the complete genomes were successfully recovered from 413, and partial genomes containing the HA segment were recovered from an additional 68 samples, which were included in the subtyping and genomic characterization.

Cohort Demographics and Clinical Outcomes

Of the 2024–2025 cohort with typed genomes, clinical metadata was available for the entire cohort of 481 unique patients (Table 1). The most represented age group was 5–17 years, which was consistent for patients infected with A(H1N1)pdm09 (28.7%) and A(H3N2) (31.0%) (Table 1). Lung disease (32.2%), immunosuppression (26.2%), and cancer (26.0%) were the most observed comorbidities (Table 1). The most common symptoms (available for a total of 439 patients) were nonspecific flu-like illness (31.2%) and fever (30.3%) (Table 1). Of the total cohort of 481 patients, 136 (28.3%) were admitted (Table 1). Notably, A(H1N1)pdm09 was associated with more hospital admissions (31.0% vs 25.0%), intensive care unit (ICU) admission (9.0% vs 4.2%), supplemental oxygen (20.5% vs 13.6%), and death (1.5% vs 0.5%) when compared to A(H3N2) (Table 1).

Hemagglutinin Gene Analysis

Among IAV–positive samples, A(H1N1)pdm09 represented a slight majority, accounting for 55.7% (268/481) (Table 2). The predominant clade within A(H1N1)pdm09 was 6B.1A.5a.2a.1, identified in 75.0% (201/268) of cases, followed by 6B.1A.5a.2a at 25.0% (67/268). Within the 6B.1A.5a.2a.1 clade, D.3 was the most frequently observed subclade, comprising 99.0% (199/201) of sequences, while subclades D.1 and D.5 were each detected in a single sample (0.5%). Within the 6B.1A.5a.2a clade, most of the sequences belonged to the C.1.9.3 subclade (83.6%; 56/67), followed by C.1.9.1 (14.9%; 10/67) and C.1.9 (1.5%; 1/67) (Table 2). A(H3N2) accounted for 44.3% (213/481) of IAV–positive samples and was exclusively classified under the 3C.2a1b.2a.2a.3a.1 clade. J.2 was the predominant subclade accounting for 90.1% (192/213)

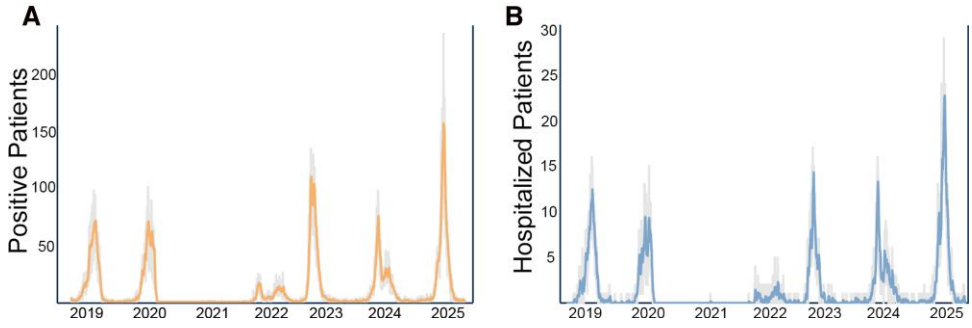

Figure 1. (*A*) Influenza A virus positives and (*B*) hospital admissions, the Johns Hopkins Health System (JHHS). Data shown as 7-d running average for positives and admissions between 17 October 2018 and 15 June 2025. Colored lines indicate the running 7-d average, and the background gray bars indicate daily cases. Dashboard; Johns Hopkins University.

Table 1. Cohort Demographics, Comorbidities, Outcomes, and Symptoms for Patients With Typed Influenza A Genomes, the 2024–2025 Influenza Season

	IAV 481	A(H1N1) 268 (55.7)	A(H3N2) 213 (44.3)
Sex, N (%)			
Female	233 (48.4%)	132 (49.2%)	101 (47.4%)
Male	248 (51.6%)	136 (50.7%)	112 (52.5%)
Age range (%)			
<2	74 (15.4%)	37 (13.8%)	37 (17.4%)
2–4	70 (14.6%)	40 (14.9%)	30 (14.1%)
5–17	143 (29.7%)	77 (28.7%)	66 (31.0%)
18–44	84 (17.5%)	38 (14.2%)	46 (21.6%)
45–64	67 (13.9%)	47 (17.5%)	20 (9.4%)
65–79	34 (7.1%)	21 (7.8%)	13 (6.1%)
80+	8 (1.7%)	7 (2.6%)	1 (0.5%)
N/A[a]	1 (0.2%)	1 (0.4%)	0 (0%)
Comorbidities, N (%)			
Hypertension	116 (24.1%)	73 (27.2%)	43 (20.2%)
Pregnancy	8 (1.7%)	2 (0.7%)	6 (2.8%)
Lung disease	155 (32.2%)	80 (30.0%)	75 (35.2%)
Kidney disease	94 (19.5%)	63 (23.5%)	31 (14.6%)
Immunosuppression	126 (26.2%)	78 (29.1%)	48 (22.5%)
Diabetes	65 (13.5%)	42 (15.7%)	23 (10.7%)
Heart failure	29 (6.0%)	15 (5.6%)	14 (6.6%)
Cancer	125 (26.0%)	77 (28.8%)	48 (22.5%)
Smoker	67 (13.9%)	41 (15.3%)	26 (12.2%)
Outcome, N (%)			
Admitted	136 (28.3%)	83 (31.0%)	53 (25.0%)
ICU	33 (6.9%)	24 (9.0%)	9 (4.2%)
Supplemental oxygen	84 (17.5%)	55 (20.5%)	29 (13.6%)
Death	5 (1.0%)	4 (1.5%)	1 (0.5%)
Total	481	268	213
Symptoms, N (%)	439	238	191
Fever	133 (30.3%)	77 (32.3%)	56 (29.3%)
Cough	35 (8.0%)	19 (7.9%)	16 (8.4%)
Headache	9 (2.1%)	3 (1.3%)	6 (3.1%)
Breathing problems	37 (8.4%)	23 (9.7%)	14 (7.3%)
Chest pain	15 (3.4%)	4 (1.7%)	11 (5.8%)
Sore throat	9 (2.1%)	4 (1.3%)	5 (2.6%)
Upper respiratory infection	17 (3.9%)	8 (3.4%)	9 (4.7%)
Abdominal pain	14 (3.2%)	7 (2.9%)	7 (3.7%)
Emesis	14 (3.2%)	10 (4.2%)	4 (2.1%)
Flu-like symptoms	137 (31.2%)	76 (31.9%)	61 (32.0%)
Seizures	15 (3.4%)	8 (3.4%)	7 (3.7%)

[a]Age unavailable for 1 patient.

Table 2. Clades and Subclades of Influenza A Virus and Their Defining Substitutions of Genomes Characterized During the 2024–2025 Season

	Number of Samples (% Cohort)	% Type, Clade, or Subclade
A(H1N1)pdm09		
Total	268	55.7
6B.1A.5a.2a (K54Q, E224A, R259K)	67	25.0
C.1.9.3 (HA1:S83P) (HA2:183T)	56	83.6
C.1.9.1 (HA1:P137S)	10	14.9
C.1.9 (HA1:T120A, K169Q)	1	1.5
6B.1A.5a.2a.1 (P137S, K142R, T216A, D260E, T277A, HA2:N124H)	201	75.0
D.1 (HA1:R45K) (nt:T1688A)	1	0.5
D.3 (HA1:T120A)	199	99.0
D.5 (HA1:R45K)	1	0.5
A(H3N2)		
Total	213	44.3
3C.2a1b.2a.2a.3a.1 (I140K)	213	100
J.2 (HA1:K276E, N122D)	192	90.1
J.2.1 (HA1:F79L, P239S)	6	2.8
J.2.2 (HA1:S124N)	15	7.0

of the A(H3N2) sequences. Subclades J.2.2 and J.2.1 were observed at 7% (15/213) and 2.8% (6/213), respectively (Table 2).

2023–2024 and 2024–2025 A(H1N1)pdm09 HA Analysis as Compared to the Egg-based A/Victoria/4897/2022 Vaccine Strain

A comparative sequence analysis was performed using 303 A(H1N1)pdm09 HA segment sequences characterized at the JHH during the 2023–2024 season [10]. Since A(H1N1)pdm09 egg-based vaccine strain (A/Victoria/4897/2022) remained unchanged between the 2023–2024 and 2024–2025 seasons, its HA sequence was used as a reference to evaluate genetic and potential antigenic divergence. The 2-season phylogenetic analysis demonstrated that the 2023–2024 6B1A.5a.2a.1 HA sequences clustered closely with A/Victoria/4897/2022. In contrast, the 2024–2025 6B1A.5a.2a.1 clinical specimens were observed to be more phylogenetically distant (Figure 2*A*). Additionally, the 2024–2025 6B1A.5a.2a clade viruses clustered distant from the sequences of the same clade from the previous influenza season.

When compared to A/Victoria/4897/2022, 132 unique AAS were found in the 2023–2024 cohort, and 128 were found in the 2024–2025 cohort. Among these, the 5 key AAS identified in the 2024–2025 season were R113K and T120A in HA1 and I45V, I133T, and V193A in HA2 (Figure 2*B*).

Each key AAS had a 2024–2025 prevalence of over 40% and more than 100% increase compared to the previous season. R113K, I45V, I133T, and V193A were exclusively found in 6B1A.5a.2a.1. In contrast, T120A was found in both 6B1A.5a.2a.1 and 6B1A.5a.2a. R113K, located near the Sa antigenic site, increased to 45% prevalence. T120A, situated within the receptor-binding site [20], reached a prevalence of 99%. The largest increases were observed in amino acid positions V193A and I133T of the HA2 gene. Notably, I133T was not identified in sequences from the 2023–2024 season but reached a prevalence of 73% in the 2024–2025 season (Figure 2*B*).

The 2023–2025 A(H1Npdm09) Hemagglutinin Nextstrain Analysis as Compared to A/Wisconsin/588/2019 as Reference Strain

The HA1 subunit of HA contains the dominant antigenic sites and was therefore the focus of our temporal analysis. Using

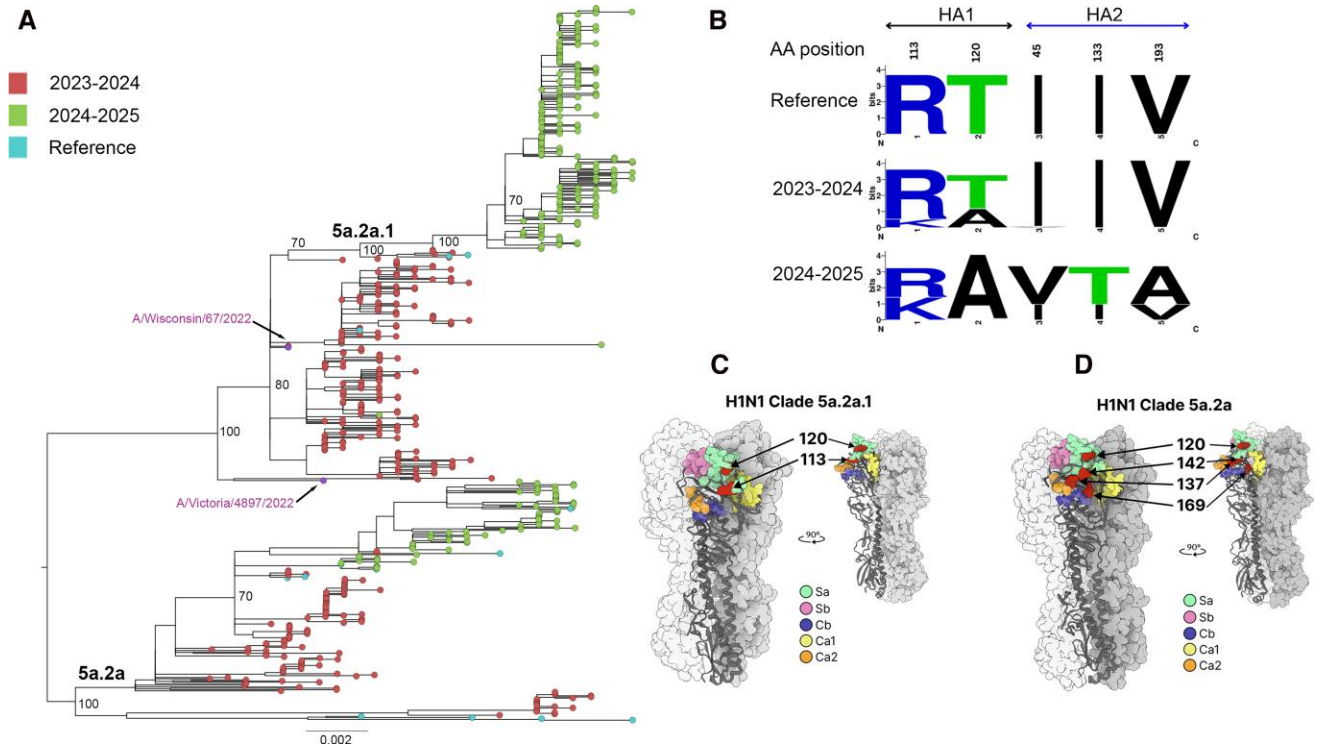

Figure 2. *A,* Phylogenetic analysis of 2023–2024 and 2024–2025 seasons A(H1N1)pdm09 hemagglutinin (HA) segments in relation to the egg-based vaccine strain A/Victoria/4897/2022 (bootstrap values detailed in Supplementary Figure 4A). *B,* Amino acid substitutions defined by a percentage increase > 100 when compared to their prevalence during the 2023–2024 season and >40% prevalence in the 2024–2025 season. Egg-based vaccine strain A/Victoria/4897/2022 used as reference. (*C*) 5a.2a.1 and (*D*) 5a.2a monomers with antigenic sites colored as Sa: Sb: Cb: Ca1: Ca2: and amino acid changes in red.

phylogenetic trees generated through Nextstrain, we identified 4 amino acids located at or near antigenic sites or receptor-binding sites [20, 21] that exhibited high entropy from October 2023 to April 2025: T120A, P137S, R142K, and K169Q (Supplementary Figure 2). T120A exhibited the highest entropy, with alanine (A) rapidly displacing threonine (T) by the end of the 2024–2025 season (T120A: 90% in October 2024 and 98% in April 2025) (Supplementary Figure 2) in both clade 5a.2a.1 and clade 5a.2a. Frequencies of other AAS in October 2024 and April 2025 were as follows: P137S, 84% and 89%; P142K, 29% and 24%; and K169Q, 27% and 24%. The 4 HA1 HA mutations were then mapped on the 3D structure of the HA1 HA protein, and their location to known antigenic sites was determined in both HA clades (Figure 2*C* and 2*D*). Three mutations were located near antigenic sites, with T120A located near antigenic site Cb, R142K at Ca2, and K169Q at Ca1 [20, 22]. Taken together, the data indicate that H1 HA proteins from the 2 dominant circulating clades were both accumulating mutations near antigenic sites.

2024–2025 A(H1N1) Clinical Isolates and Reduced Neutralization Using Sera From Adult Healthcare Workers

To evaluate the impact of HA mutations on escape from preexisting and vaccine-induced neutralizing antibodies, virus stocks of A(H1N1)pdm09 clades 5a.2a and 5a.2a.1 were generated. The 2024–2025 A(H1N1) vaccine strain (A/Victoria/4897/2022) was propagated as a comparator. Serum neutralizing activity was assessed using pre- and postvaccination sera from 50 adults enrolled in the JH-CEIRR annual influenza vaccine cohort (Supplementary Table 3).

Pre- and postvaccination sera neutralized the vaccine strain more efficiently than either clade 5a.2a or 5a.2a.1 viruses (Figure 3*A* and 3*B*). Fold increases in neutralizing titers (1.9–2.6) did not differ significantly among viruses (Figure 3*C*), and seroconversion rates (>4-fold increase) were similar across vaccine and clinical isolates. Although postvaccination neutralizing titers were lower against clinical isolates than against the vaccine strain, the relative pre- to postvaccination increase was greater for the clinical isolates (Figure 3*D*). Among clade 5a.2a.1 viruses, a K substitution at residue 113 was neutralized less efficiently than the parental R substitution (Figure 3*D*).

2023–2024 and 2024–2025 A(H3N2) HA Analysis as Compared to the A/Darwin/6/2021 on Nextstrain

All A(H3N2) HA sequences belonged to the 3C.2a1b.2a.2a.3a.1 clade, represented by subclades J.2 (90.2%), J.2.1 (2.8%), and J.2.2 (7%) (Table 2). Sequences from the 2024–2025 clinical samples were clustered with the egg- and cell-based vaccine

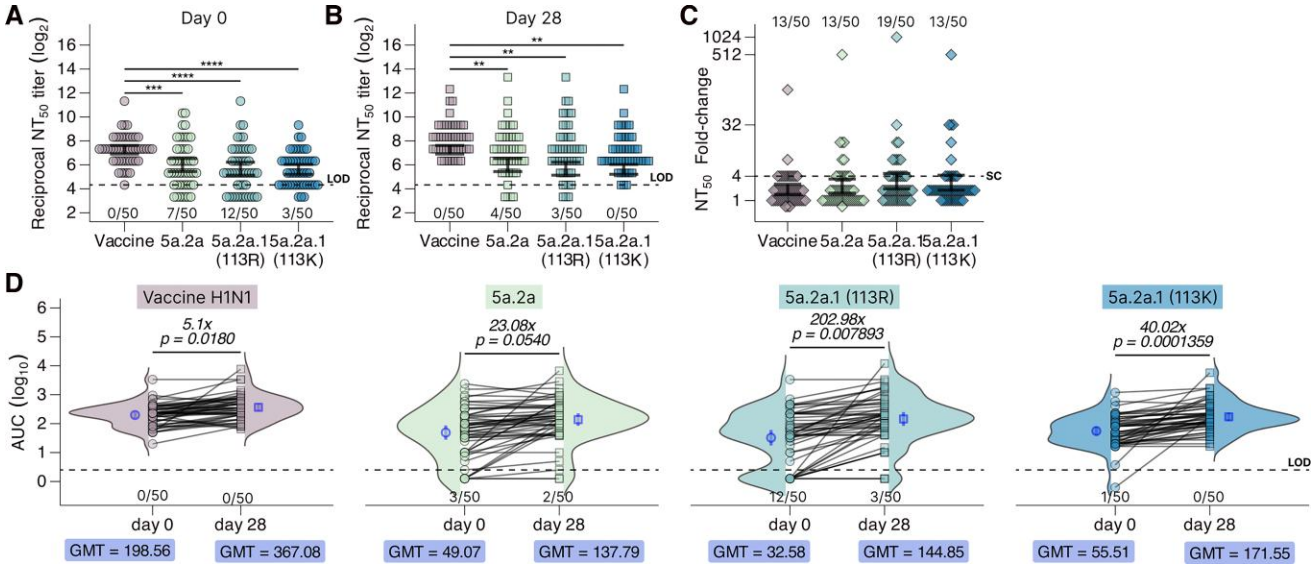

Figure 3. The 2024–2025 A(H1N1) influenza A virus (IAV) escape from serum neutralizing activity before and after vaccination. Serum neutralizing antibody titers (NT50; mean ± standard error) were measured: (*A*) At baseline (day 0) and (*B*) 28 d postvaccination, against the 2024–2025 A/H1N1 vaccine strain A/Victoria/4897/2022. Three representative 2024–2025 circulating viruses were tested in parallel: 1 5a.2a clade virus (A/Baltimore/JH-250/2025) and 2 5a.2a.1 clade viruses (A/Baltimore/JH-260/2025 and A/Baltimore/JH-305/2025), selected based on amino acid identity at position 113 (H1N1 numbering). For each virus, the number of seronegative individuals is shown as n/N below the corresponding data points. *C*, Fold change in NT50 from day 0 to day 28 was used to assess seroconversion, defined as NT50 ≥ 4-fold increase. The fraction of individuals who seroconverted (n/50) is shown above each data group. The dotted line denotes the limit of detection (LOD; NT50 at the starting dilution of 1:20). Samples with no detectable neutralization are plotted at one-half the LOD. *D*, Area under the curve (AUC) values at day 0 and day 28 are shown, with an LOD of 2.5. Fold changes in AUC are indicated above paired data points. The number of seronegative individuals (n/N) is shown beneath each virus group. Statistical comparisons within or between nontransformed NT50 and AUC values were performed using paired Wilcoxon tests with Bonferroni post hoc correction. Adjusted *P*-values or a corresponding symbol are shown above significant comparisons: 0.1234 (ns), .332(*), .0021(**), .0002(***), <.00001(****).

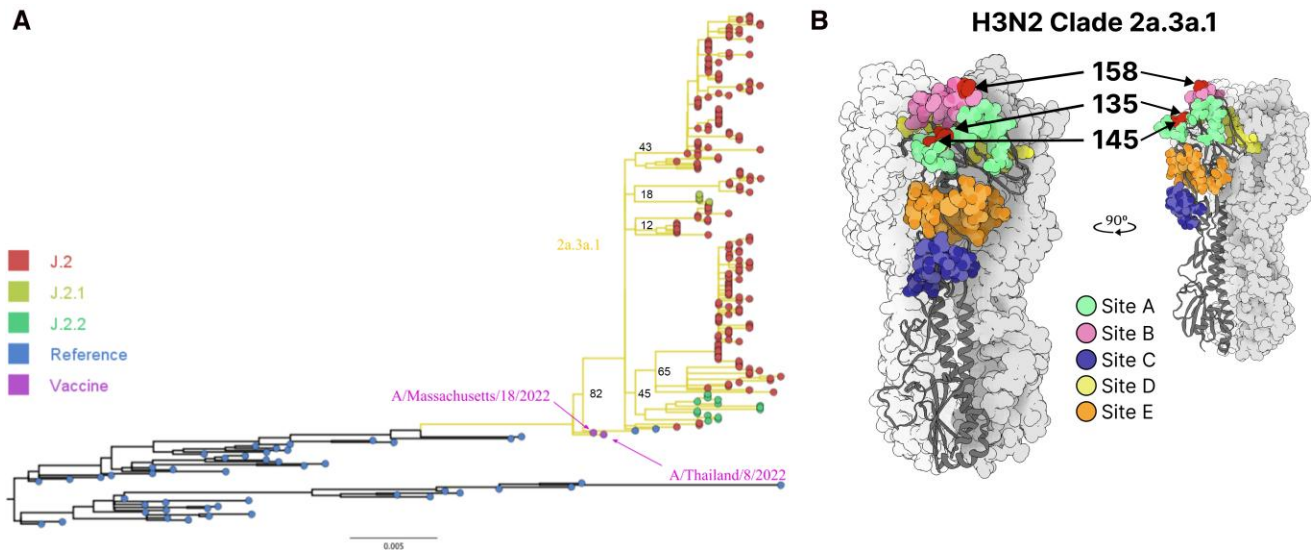

Figure 4. *A*, Phylogenetic analysis of 2023–2024 and 2024–2025 seasons H3N2 hemagglutinin (HA) segments in relation to strain A/Darwin/6/2021 (bootstrap values detailed in Supplementary Figure 4B). *B*, A(H3N2) clade 2a.3a.1 monomers with antigenic sites colored. Amino acid changes are shown in red.

strains A/Thailand/8/2022 and A/Massachusetts/18/2022 [23], respectively, but did form distinct branches, indicating genetic evolution (Figure 4*A*).

Three specific amino acid changes began to gain prevalence during the 2024–2025 season—T135K, S145N, and N158K—with frequencies in October 2024 and April 2025 as follows:

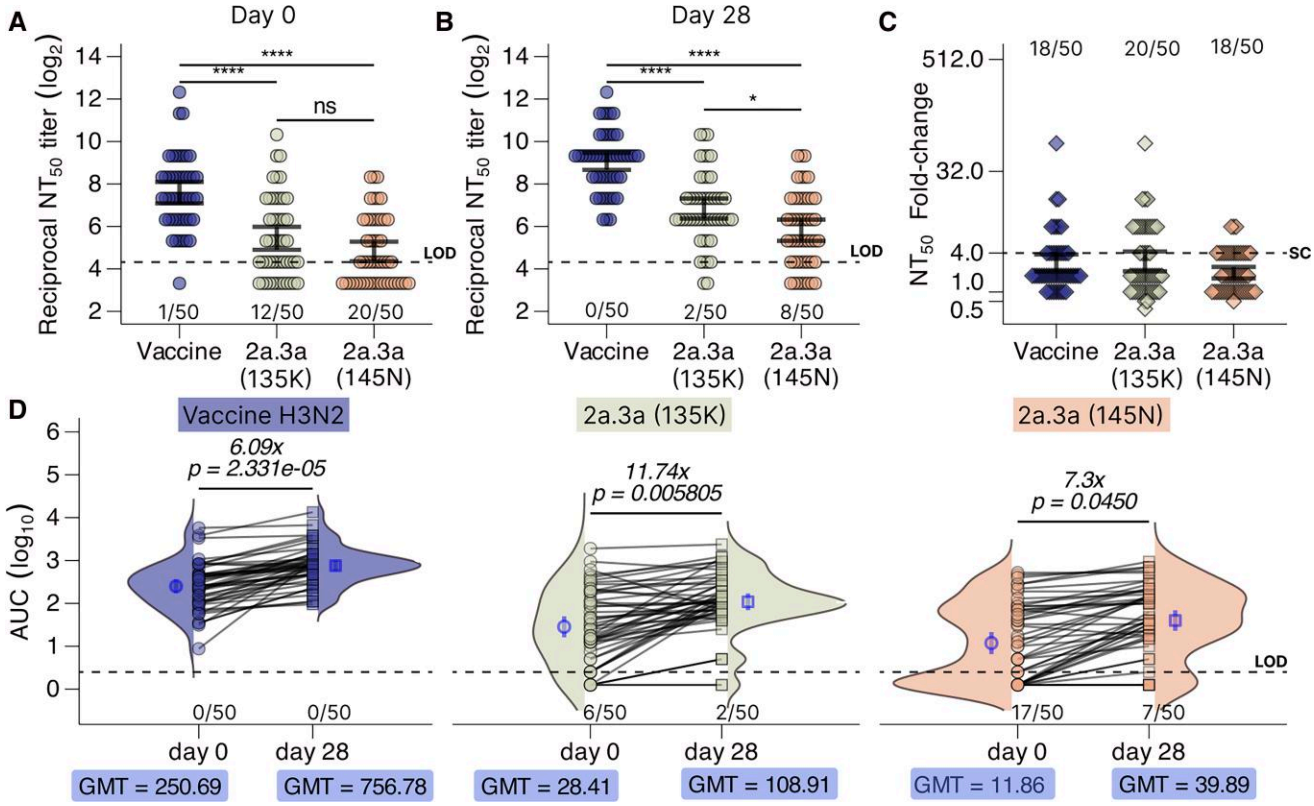

Figure 5. The 2024–2025 A(H3N2) IAV escape from serum neutralizing activity before and after vaccination. Serum neutralizing antibody titers (NT50; mean ± standard error) were measured: (*A*) At baseline (day 0) and (*B*) 28 d postvaccination, against the 2024–25 A/H3N2 vaccine strain A/California/122/2022. Two representative 2024–2025 circulating viruses belonging to clade 3a.1 subclade J.2 were tested in parallel. Each strain encoded HA1 mutations we hypothesize to contribute toward antigenic drift. These strains included A/Baltimore/JH-610/2025 (encoding HA1: **T135K**) and A/Baltimore/JH-588/2025 (encoding HA1: **S145N** and N158K). Bolded mutations corresponded to the virus labels within each panel. For each virus, the number of seronegative individuals is shown as *n/N* below the corresponding data points. *C*, Fold change in NT50 from day 0 to day 28 was used to assess seroconversion, defined as NT50 ≥ 4-fold increase. The fraction of individuals who seroconverted (*n/50*) is shown above each data group. The dotted line denotes the limit of detection (LOD; NT50 at the starting dilution of 1:20). Samples with no detectable neutralization are plotted at one-half the LOD. *D*, Area under the curve (AUC) values at day 0 and day 28 are shown, with an LOD of 2.5. Fold changes in AUC are indicated above paired data points. The number of seronegative individuals (*n/N*) is shown beneath each virus group. Statistical comparisons within or between nontransformed NT50 and AUC values were performed using paired Wilcoxon tests with Bonferroni post hoc correction. Adjusted *P*-values or a corresponding symbol are shown above significant comparisons: 0.1234 (ns), .332(*), .0021(**), .0002(***), <.00001(****).

T135K, 26% and 33%; S145N, 43% and 50%; and N158K, 26% and 36% (Supplementary Table 3). These amino acids emerged in slightly different subclades, with T135K and N158K accumulating only in the J.2 subclade, while S145N emerged in both J.2 and J.2.2.

Mapping these 3 mutations on the structure of the H3 HA protein (Figure 4*B*) demonstrated that each occurred at or near an antigenic site, with N158K near site B and S145N and T135K in antigenic site A [22].

2024–2025 A(H3N2) Clinical Isolates and Reduced Neutralization Using Sera From Adult Healthcare Workers

To assess the impact of HA mutations on escape from preexisting neutralizing antibodies, virus isolates were generated for A/H3N2 clade 2a.3a.1, subclade J.2.2 (N158K and S145N) and subclade J.2 (T135K). The 2024–2025 A(H3N2) vaccine strain (A/California/122/2022), antigenically similar to A/Thailand/8/2022 [24], was propagated as a comparator. Pre- and postvaccination sera from the H1 neutralization panel were used to evaluate neutralizing activity (Supplementary Table 3).

Both pre- and postvaccination sera neutralized the vaccine strain more efficiently than either mutant virus (Figure 5*A* and 5*B*), indicating that the N158K, S145N, and T135K mutations contributed to reduced neutralization. Seroconversion rates (Figure 5*C*) and postvaccination fold increases (Figure 5*D*) did not differ significantly among viruses.

Neuraminidase Gene Analysis

Of the 648 samples selected for sequencing, high-quality NA segments were recovered from 476 IAV. Neuraminidase clade designations are referred herein according to Nextstrain nomenclature available at https://github.com/influenza-clade-nomenclature (accessed 16 August 2025). Among A(H1N1) pdm09, 265 NA segments were clustered into 2 clades:

C.5.3.1 was predominant, representing 90.9% (241/265), while C.5.3 accounted for 9.1% (24/265) (Supplementary Table 4). The most common HA subclade, D.3, typically clustered with NA clade C.5.3.1, though some sequences were also associated with C.5.3.

For A(H3N2), 211 NA sequences were recovered, most (97.2%; 205/211) belonged to the B.4.2 clade, with the remaining 2.8% (6/211) classified as B.4 clade (Supplementary Table 4). Our A(H3N2) NA phylogenetic analysis highlights the high prevalence of the B.4.2 clade. The less common B.4 clade was found exclusively in sequences associated with HA subclade J.2.1 (Supplementary Table 4).

Several AAS associated with NA inhibitor resistance were identified. S247N was encountered in 13.9% (34/241) of A(H1N1)pdm09 samples within the C.5.3.1 clade. However, the additional I223V substitution typically required in combination with S247N for reduced oseltamivir susceptibility [25] was not observed in the same samples. Instead, I223V was identified by itself in a single sample. The H275Y substitution, well characterized to confer oseltamivir resistance [26], was identified in only 2 N1 samples (Supplementary Table 5). No mutations in the N2 NA protein associated with antiviral resistance were identified.

CONCLUSIONS

According the Centers for Disease Control and Prevention (CDC), the 2024–2025 influenza season in the United States was associated with higher incidence and emergency department admission rates than the prior season [27]. Genomic analysis of viruses characterized at JHHS showed that this increase coincided with substantial cocirculation of A(H1N1)pdm09 and A(H3N2). While our findings align with national positivity trends, it is important to note that genome recovery from nasopharyngeal specimens depends on viral load, introducing potential selection bias.

A(H1N1)pdm09 clades 5a.2a and 5a.2a.1 cocirculated, with both accumulating mutations at or near antigenic sites. A(H3N2) prevalence was markedly higher than in the previous season [10], accounting for nearly half of IAV–positive cases. All H3 HA sequences belonged to clade 3C.2a1b.2a.2a.3a.1, in contrast to the prior season, which also included low-level circulation of 3C.2a1b.2a.2b. Using pre- and postvaccination sera, we demonstrated antigenic drift in both A(H1N1)pdm09 and A(H3N2) clinical isolates, indicating that observed HA genetic changes altered antigenic properties.

Immunologic and sequence analyses indicated that mutations in key HA codons reduced serum neutralization. In A(H1N1)pdm09, T120A (near antigenic site Cb) and R113K (near site Sa) were frequently observed and were associated with reduced neutralization relative to egg-based vaccine strains. The P137S substitution within the receptor-binding site may enhance viral attachment, potentially contributing to increased transmissibility or virulence [20]. In A(H3N2), N158K (antigenic site B) and T135K and S145N (near antigenic site A) were associated with reduced pre- and postvaccination neutralization. S145N and N158K co-occurred in subclade J.2, while T135K was detected in both J.2 and J.2.2.

Interim vaccine effectiveness (VE) estimates during the 2023–2024 season ranged from 59% to 67% for pediatric outpatients and 52% to 61% for pediatric hospitalizations and from 33% to 49% and 41% to 44% for adult outpatients and hospitalizations, respectively [28]. During the 2024–2025 season, VE estimates from the NVSN, US Flu VE, and VISION networks ranged from 32% to 60% for pediatric outpatients, 63% to 78% for pediatric hospitalizations, and 36% to 55% and 41% to 55% for adult outpatients and hospitalizations, respectively [29]. Together, these data demonstrate continued protection against influenza-associated hospitalization among vaccinated individuals, underscoring the importance of annual vaccination and ongoing surveillance.

For the 2024–2025 Northern Hemisphere season, the WHO recommended A/Victoria/4897/2022 (Egg) and A/Wisconsin/67/2022 (Cell) for A(H1N1)pdm09, A/Thailand/8/2022 (Egg) and A/Massachusetts/18/2022 (Cell) for A(H3N2), and B/Austria/1359417/2021 for IBV [23]. For 2025–2026, the A(H1N1)pdm09 egg-based vaccine strain A/Victoria/4897/2022 was again recommended, marking its third consecutive season [30]. However, our phylogenetic and neutralization data indicate that 2024–2025 clade 5a.2a.1 viruses exhibited greater divergence from the vaccine strain than those from 2023–2024. Reduced neutralization of representative A(H1N1)pdm09 clinical isolates by sera from 2024 vaccine recipients supports ongoing antigenic drift. Similarly, the 2025–2026 A(H3N2) vaccine strain lacks the S145N, N158K, and T135K substitutions associated with reduced neutralization. Collectively, these findings indicate that the 2024–2025 egg-based vaccine strains for both A(H1N1)pdm09 and A(H3N2) lack key antigenic changes present in circulating viruses.

We also observed an increase in NA substitutions associated with reduced oseltamivir susceptibility in A(H1N1)pdm09 viruses. Notably, the S247N substitution increased from 0.33% in 2023–2024 to 13.9% in the 2024–2025 cohort [10]. Although I223V and H275Y remained infrequent, the rise in S247N highlights the need for continued antiviral resistance surveillance.

In summary, our study demonstrates ongoing genomic evolution of influenza viruses during the 2024–2025 season within the JHHS. The increased incidence of influenza-positive cases mirrored national CDC trends. Genomic analysis showed that A(H1N1)pdm09 remained the dominant subtype despite substantial cocirculation with A(H3N2). Notably, A(H1N1)pdm09 viruses carrying the NA substitution H275Y, which is well characterized to confer oseltamivir resistance, increased compared with the prior season. Although no viruses

contained both I223V and S247N, the rising frequency of S247N, together with the accumulation of substitutions in antigenic and receptor-binding sites, suggests potential effects on viral fitness and immune evasion. Collectively, these findings underscore the critical role of genomic surveillance in informing antiviral effectiveness and guiding future vaccine strain selection.

The limitations of our study include the potential bias of patients' selection due to the retrospective nature of sample collections. The metadata and outcome data were limited to patients with influenza sequencing results, which restricted statistical outcome comparisons between subclades. Serum samples collected for neutralization assays were a part of a HCW study cohort and did not include samples from age groups younger than 21 years. In contrast, the surveillance cohort was collected from a patient population that was largely younger than 18 years, which restricts the representation of population immunity. Our study focused on the genotypic analysis of the JHHS cohort only to associate the data with clinical and metadata and hence might not be nationally or globally representative.

Supplementary Data

Supplementary materials are available at *The Journal of Infectious Diseases* online (http://jid.oxfordjournals.org/). Supplementary materials consist of data provided by the author that are published to benefit the reader. The posted materials are not copyedited. The contents of all supplementary data are the sole responsibility of the authors. Questions or messages regarding errors should be addressed to the author.

Notes

Acknowledgments. The authors would like to acknowledge the staff in the JHHS medical microbiology laboratories for their aid in this study. The data underlying this article are available in the GISAID database (accession numbers, Supplementary Table 1, HA and NA FASTA files, Supplementary Datasets 1–4). D. V.: Methodology, Software, Validation, Formal analysis, Investigation, Data curation, Writing—original draft, Writing—review & editing. A. F.: Methodology, Software, Validation, Formal analysis, Investigation, Data curation, Writing—review & editing. E. A.: Methodology, Software, Validation, Formal analysis, Investigation, Data curation, Writing—original draft, Writing—review & editing. A. P. W.: Methodology, Writing—review & editing. M. P.: Methodology, Writing—review & editing. Y. V.: Methodology, Writing—review & editing. O. A.: Methodology, Writing—review & editing. T. X. Z.: Methodology, Writing—review & editing. J. M. N.: Methodology, Writing—review & editing. R. E. R.: Validation, Resources, Writing—review & editing, Visualization, Project administration, Funding acquisition. K. Z. J. F.: Resources, Project administration, Writing—review & editing. C. P. M.: Methodology, Software, Validation, Writing—review & editing. E. K.: Software, Validation, Data curation, Visualization. A. P.: Validation, Resources, Writing—review & editing, Visualization, Project administration, Funding acquisition. H. H. M.: Conceptualization, Methodology, Software, Validation, Investigation, Resources, Data curation, Writing—original draft, Writing—review & editing, Visualization, Supervision, Project administration, Funding acquisition.

Financial support. This study was funded by the Johns Hopkins Center of Excellence in Influenza Research and Response (HHS 75N93021C000045) and 5T32AI007417-25 (EHA). The views expressed in this manuscript are those of the authors and do not necessarily represent the views of the National Institute of Biomedical Imaging and Bioengineering; the National Heart, Lung, and Blood Institute; the National Institutes of Health; or the US Department of Health and Human Services.

Potential conflicts of interest. H. H. M. collaborates for research with Hologic, Qiagen, and Diasorin. H. H. M. received honoraria from Roche Diagnostics, Qiagen, Diasorin, bioMérieux, and BD Diagnostics. All other authors report no potential conflicts. All other authors report no potential conflicts.

All authors have submitted the ICMJE Form for Disclosure of Potential Conflicts of Interest. Conflicts that the editors consider relevant to the content of the manuscript have been disclosed.

References

1. Kim H, Webster RG, Webby RJ. Influenza virus: dealing with a drifting and shifting pathogen. Viral Immunol **2018**; 31:174–83.
2. Uyeki TM. High-risk groups for influenza complications. JAMA **2020**; 324:2334.
3. Hu T, Miles AC, Pond T, et al. Economic burden and secondary complications of influenza-related hospitalization among adults in the US: a retrospective cohort study. J Med Econ **2024**; 27:324–36.
4. Akin E, Villafuerte DA, Werner AP, et al. Emergence of an antigenically drifted and reassorted influenza B virus at the end of the 2024–25 influenza season. bioRxiv 666632 [Preprint]. 2025. Available at: https://doi.org/10.1101/2025.07.24.666632.
5. CDC. Influenza activity in the United States during the 2023–2024 season and composition of the 2024–2025 influenza vaccine | influenza (Flu). CDC. Available at: https://www.cdc.gov/flu/whats-new/flu-summary-2023-2024.html. Accessed October 29, 2024.
6. Mostafa HH, Carroll KC, Hicken R, et al. Multicenter evaluation of the cepheid Xpert Xpress SARS-CoV-2/Flu/RSV test. J Clin Microbiol **2021**; 59:e02955-20.

7. Jarrett J, Uhteg K, Forman MS, et al. Clinical performance of the GenMark Dx ePlex respiratory pathogen panels for upper and lower respiratory tract infections. J Clin Virol **2021**; 135:104737.
8. Quinton M, Geahr M, Gluck L, Jarrett J, Mostafa HH. Evaluation of the respiratory NeuMoDx Flu A-B/RSV/SARS-CoV-2 Vantage and Alinity m Resp-4-Plex assays. J Clin Virol **2022**; 150–151:105164.
9. Fall A, Han L, Yunker M, et al. Evolution of influenza A(H3N2) viruses in 2 consecutive seasons of genomic surveillance, 2021–2023. Open Forum Infect Dis **2023**; 10:ofad577.
10. Yunker M, Villafuerte DA, Fall A, et al. Genomic evolution of influenza during the 2023–2024 season, the Johns Hopkins Health System. J Clin Virol **2024**; 174:105718.
11. Zhou B, Donnelly ME, Scholes DT, et al. Single-reaction genomic amplification accelerates sequencing and vaccine production for classical and Swine origin human influenza a viruses. J Virol **2009**; 83:10309–13.
12. Zhou B, Lin X, Wang W, et al. Universal influenza B virus genomic amplification facilitates sequencing, diagnostics, and reverse genetics. J Clin Microbiol **2014**; 52:1330–7.
13. Yunker M, Fall A, Norton JM, et al. Genomic evolution and surveillance of respiratory syncytial virus during the 2023–2024 season. Viruses **2024**; 16:1122.
14. Hadfield J, Megill C, Bell SM, et al. Nextstrain: real-time tracking of pathogen evolution. Bioinformatics **2018**; 34: 4121–3.
15. Fall A, Abdullah O, Han L, et al. Enterovirus D68: genomic and clinical comparison of 2 seasons of increased viral circulation and discrepant incidence of acute flaccid myelitis-Maryland, USA. Open Forum Infect Dis **2024**; 11:ofae656.
16. Lee JM, Huddleston J, Doud MB, et al. Deep mutational scanning of hemagglutinin helps predict evolutionary fates of human H3N2 influenza variants. Proc Natl Acad Sci **2018**; 115:E8276–85.
17. Swanson NJ, Marinho P, Dziedzic A, et al. 2019–2020 H1N1 clade A5a.1 viruses have better in vitro fitness compared with the co-circulating A5a.2 clade. Sci Rep **2023**; 13: 10223.
18. Liu H, Shaw-Saliba K, Westerbeck J, et al. Effect of human H3N2 influenza virus reassortment on influenza incidence and severity during the 2017–18 influenza season in the USA: a retrospective observational genomic analysis. Lancet Microbe **2024**; 5:100852.
19. Swanson NJ, Girish J, Yunker M, et al. Clade-defining mutations in human H1N1 hemagglutinin protein from 2021–2023 have opposing effects on in vitro fitness and antigenic drift. bioRxiv 594815 [Preprint]. 2024. Available at: https://doi.org/10.1101/2024.05.18.594815.
20. Sriwilaijaroen N, Suzuki Y. Molecular basis of the structure and function of H1 hemagglutinin of influenza virus. Proc Jpn Acad Ser B Phys Biol Sci **2012**; 88:226–49.
21. Wang MH, Lou J, Cao L, et al. Characterization of key amino acid substitutions and dynamics of the influenza virus H3N2 hemagglutinin. J Infect **2021**; 83:671–7.
22. Stray SJ, Pittman LB. Subtype- and antigenic site-specific differences in biophysical influences on evolution of influenza virus hemagglutinin. Virol J **2012**; 9:91.
23. Recommended composition of influenza virus vaccines for use in the 2024–2025 northern hemisphere influenza season. 23 February 2024 Meeting report. Available at: https://www.who.int/publications/m/item/recommended-composition-of-influenza-virus-vaccines-for-use-in-the-2024-2025-northern-hemisphere-influenza-season. Accessed 14 February 2026.
24. https://cdn.who.int/media/docs/default-source/influenza/cvvs/cvv-northern-hemisphere-2024-2025/a_h3n2_cvv-egg_nh24-25.pdf?sfvrsn=363ee66f_11. Accessed 14 February 2026.
25. Patel MC, Nguyen HT, Pascua PNQ, et al. Multicountry spread of influenza A(H1N1)pdm09 viruses with reduced oseltamivir inhibition, May 2023-February 2024. Emerg Infect Dis **2024**; 30:1410–5.
26. Brookes DW, Miah S, Lackenby A, Hartgroves L, Barclay WS. Pandemic H1N1 2009 influenza virus with the H275Y oseltamivir resistance neuraminidase mutation shows a small compromise in enzyme activity and viral fitness. J Antimicrob Chemother **2011**; 66:466–70.
27. Respiratory Virus Activity Levels. Available at: https://www.cdc.gov/respiratory-viruses/data/activity-levels.html. Accessed 14 February 2026.
28. Frutos AM, Price AM, Harker E, et al. Interim estimates of 2023–24 seasonal influenza vaccine effectiveness—United States. MMWR Morb Mortal Wkly Rep **2024**; 73:168–74.
29. Frutos AM, Cleary S, Reeves EL, et al. Interim estimates of 2024–2025 seasonal influenza vaccine effectiveness—four vaccine effectiveness networks, United States, October 2024-February 2025. MMWR Morb Mortal Wkly Rep **2025**; 74:83–90.
30. Recommended composition of influenza virus vaccines for use in the 2025–2026 northern hemisphere influenza season. Available at: https://www.who.int/publications/m/item/recommended-composition-of-influenza-virus-vaccines-for-use-in-the-2025-2026-nh-influenza-season. Accessed 14 February 2026.